MICROBES AND ENVIRONMENTS

Geochemical and Microbiological Evidence for Microbial Methane Production in Deep Aquifers of the Cretaceous Accretionary Prism

Makoto Matsushita[1], Kenta Magara[2], Yu Sato[1], Naoya Shinzato[3], and Hiroyuki Kimura[1,2,4,5]*

[1]Department of Environment and Energy Systems, Graduate School of Science and Technology, Shizuoka University, 836 Oya, Suruga-ku, Shizuoka 422–8529, Japan; [2]Department of Science, Graduate School of Integrated Science and Technology, Shizuoka University, 836 Oya, Suruga-ku, Shizuoka 422–8529, Japan; [3]Tropical Biosphere Research Center, Ryukyus University, 1 Senbaru, Nishihara, Okinawa 903–0213, Japan; [4]Department of Geosciences, Faculty of Science, Shizuoka University, 836 Oya, Suruga-ku, Shizuoka 422–8529, Japan; and [5]Research Institute of Green Science and Technology, Shizuoka University, 836 Oya, Suruga-ku, Shizuoka 422–8529, Japan

Accretionary prisms are thick layers of sedimentary material piled up at convergent plate boundaries. Large amounts of anaerobic groundwater and methane (CH_4) are contained in the deep aquifers associated with accretionary prisms. In order to identify microbial activity and CH_4 production processes in the deep aquifers associated with the Cretaceous accretionary prism in Okinawa Island, Japan, we performed geochemical and microbiological studies using anaerobic groundwater and natural gas (mainly CH_4) samples collected through four deep wells. Chemical and stable hydrogen and oxygen isotope analyses of groundwater samples indicated that the groundwater samples obtained from each site originated from ancient seawater and a mixture of rainwater and seawater, respectively. Additionally, the chemical and stable carbon isotopic signatures of groundwater and natural gas samples suggested that CH_4 in the natural gas samples was of a biogenic origin or a mixture of biogenic and thermogenic origins. Microscopic observations and a 16S rRNA gene analysis targeting microbial communities in groundwater samples revealed the predominance of dihydrogen (H_2)-producing fermentative bacteria and H_2-utilizing methanogenic archaea. Moreover, anaerobic cultures using groundwater samples suggested a high potential for CH_4 production by a syntrophic consortium of H_2-producing fermentative bacteria and H_2-utilizing methanogenic archaea through the biodegradation of organic substrates. Collectively, our geochemical and microbiological data support the conclusion that the ongoing biodegradation of organic matter widely contributes to CH_4 production in the deep aquifers associated with the Cretaceous accretionary prism.

Key words: accretionary prism, deep aquifer, methanogenic archaea, fermentative bacteria, syntrophic consortium

Accretionary prisms are thick layers of sedimentary material piled up at convergent plate boundaries. These materials originated from ancient marine sediments that were deposited on a subducting ocean plate and accreted onto a non-subducting continental plate (47). Accretionary prisms are found in large regions of the world, including Alaska and Washington in the U.S., New Zealand, Chile, Peru, Indonesia, Taiwan, Russia, and Japan (15, 19, 23, 26).

The Shimanto Belt in southwest Japan is a typical and highly studied accretionary prism. The Shimanto Belt was mainly formed during the Cretaceous and Paleogene Periods and originated from ancient marine sediments that were deposited on the Philippine Sea Plate (23). These sediments are approximately 10 km thick and traceable laterally for 1,800 km in parallel with the Nankai Trough and Ryukyu Trench (Fig. 1A) (46). They are mainly composed of non- to weakly metamorphosed sequences of sandstone, mudstone, chert, and greenstone. Groundwater is primarily recharged by rainwater and seawater that infiltrates into outcrops or faults, then flows down through permeable sandstone and is anaerobically reserved in deep aquifers. In addition to anaerobic groundwater, a high concentration of natural gas, mainly methane (CH_4), is contained in deep aquifers (27, 32, 43).

It is generally accepted that the origin of CH_4 in natural gas

reserves in subsurface sedimentary deposits is either biogenic (formed by methanogenic archaea) or thermogenic (formed by the thermal degradation of organic matter in sedimentary layers). Previous studies performed a series of geochemical and microbiological analyses of anaerobic groundwater and natural gas derived from deep aquifers of the Paleogene accretionary prism distributed in southwest Japan. Based on their findings, these studies suggested a syntrophic consortium model in deep aquifers, in which the anaerobic biodegradation of organic matter in the sediment mediated by H_2-producing fermentative bacteria and H_2-utilizing methanogenic archaea contribute to CH_4 production (4, 27, 32).

The anaerobic deep aquifers associated with accretionary prisms are considered to contain large amounts of CH_4. This CH_4 is a potential greenhouse gas and important energy resource. However, all of the research on the CH_4 production process conducted to date has targeted the Paleogene accretionary prism. Although Cretaceous accretionary prisms are also distributed across large regions of the world, microbial activity and CH_4 production processes in the deep aquifers of older accretionary prisms remain unknown.

Therefore, the objectives of the present study were to reveal the microbial activity and CH_4 production process in deep aquifers associated with the Cretaceous accretionary prism in Okinawa Island, Japan. We collected anaerobic groundwater and natural gas samples derived from deep aquifers through deep wells, and subjected them to a series of

* Corresponding author. E-mail: kimura.hiroyuki@shizuoka.ac.jp;
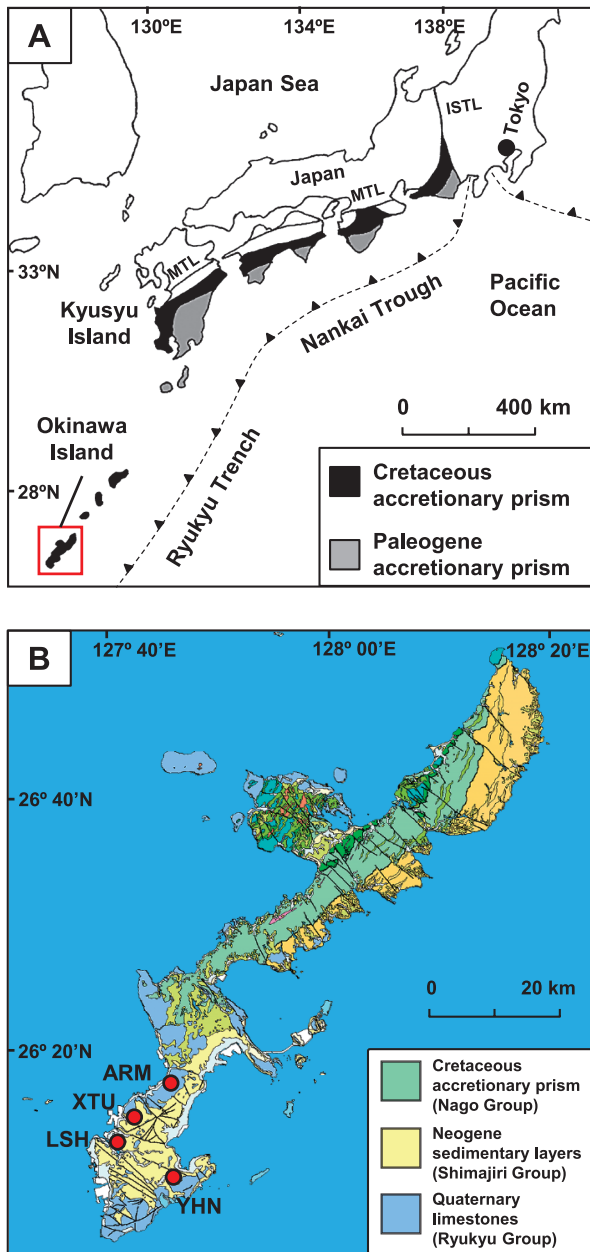 Tel: +81–54–238–4784; Fax: +81–54–238–0491.

Fig. 1. (A) The location of the accretionary prism in Japan, known as the Shimanto Belt, and (B) geological map of the study area (red square). The location of the Shimanto Belt was taken from Kano *et al.* (23). The geological map is modified from a 1:200,000 seamless digital geological map of Japan (16). The red circles indicate the location of the wells used for sampling. MTL, Median Tectonic Line; ISTL, Itoigawa-Shizuoka Tectonic Line.

geochemical and microbiological analyses. The microbial activity and CH_4 production process revealed in the present study were compared with those previously reported in deep aquifers of the Paleogene accretionary prism.

Materials and Methods

Study site and sample collection

Okinawa Island has an area of 1,207 km² and is located approximately 640 km south of Kyusyu Island, Japan (Fig. 1A). The accretionary prism known as the Nago Group (mainly Cretaceous) in the

Shimanto Belt is distributed over the island (Fig. 1B) (35, 50). The Nago Group is composed principally of sandstone, mudstone, and greenstone. In the southern part of Okinawa Island, the sedimentary layers referred to as the Shimajiri Group (mainly Neogene) unconformably overlay the Nago Group (49). The Shimajiri Group is composed mainly of sandstone, mudstone, and tuff, and is unconformably covered with Quaternary limestone (the Ryukyu Group).

Anaerobic groundwater and natural gas samples derived from deep aquifers in the Nago Group were collected through four deep wells: YHN, LSH, XTU, and ARM (Fig. 1B). These wells were drilled down to 800–2,119 m and reached deep aquifers in the Nago Group (Table S1) (25, 49). As well strainers extend over the Nago and Shimajiri Groups at the YHN site, samples may also contain groundwater and natural gas derived from the Shimajiri Group.

Groundwater at these wells is anaerobically drawn up to ground level by a water pump or by natural water pressure. In the present study, groundwater was pumped for more than 24 h before sampling in order to prevent contamination by air and water from shallow environments. Groundwater samples were collected under anaerobic conditions into autoclaved serum bottles and polycarbonate bottles using a sterile silicone tube. The concentrations of dissolved natural gas were so high that gas exsolved at the ground level. Natural gas samples were collected into autoclaved serum bottles underwater in order to prevent contamination by air. Serum bottles were tightly sealed with sterile butyl-rubber stoppers and aluminum crimps.

Physicochemical and stable isotope analyses of groundwater and natural gas

We measured the temperature, pH, oxidation-reduction potential (ORP), and electrical conductivity (EC) of groundwater samples at the outflow of the wells. The concentrations of cations (Na^+, Ca^{2+}, Mg^{2+}, K^+, and NH_4^+) and anions (Cl^-, Br^-, I^-, F^-, PO_4^{3-}, NO_3^-, SO_4^{2-}, HCO_3^-, acetate, and formate) in groundwater were analyzed using an ICS-1500 ion chromatography system (Dionex, Sunnyvale, CA, USA). Sulfide was analyzed using a No. 211 sulphide ion detector tube (Gastec, Kanagawa, Japan). Dissolved organic carbon (DOC) was measured on a TOC-V total organic carbon analyzer (Shimadzu, Kyoto, Japan). The concentrations of natural gas components (H_2, N_2, O_2, CO_2, CH_4, C_2H_6, C_3H_8, and C_4H_{10}) were analyzed on a GC-2014 gas chromatograph equipped with a thermal conductivity detector and flame ionization detector (Shimadzu) following the procedures described by Matsushita *et al.* (32). The detection limits of the analysis were 0.01 vol.% for H_2, N_2, O_2, CO_2, and CH_4, and 0.001 vol.% for C_2H_6, C_3H_8, and C_4H_{10}.

The stable hydrogen and oxygen isotope ratios of groundwater samples (D/H and $^{18}O/^{16}O$) were measured on a DLT-100 liquid water isotope analyzer (Los Gatos Research, San Jose, CA, USA) (13). The stable carbon isotope ratio ($^{13}C/^{12}C$) of dissolved inorganic carbon (DIC; consisting mainly of HCO_3^-) was analyzed as described previously (36). Groundwater samples for analyzing the $^{13}C/^{12}C$ of DIC were fixed with 0.5 mL of saturated $HgCl_2$ solution and sealed with sterile butyl-rubber stoppers and aluminum crimps with no air bubbles. A 10-mL headspace was created inside each serum bottle with pure helium gas and acidified by adding CO_2-free H_3PO_4 solution. Sample bottles were left in the dark for 24 h in order to achieve equilibrium between dissolved CO_2 and headspace CO_2. CO_2 in this headspace was subsampled, and the $^{13}C/^{12}C$ ratio of CO_2 was measured with a Trace GC Ultra gas chromatograph (Thermo Fisher Scientific) that was connected to a Delta^{plus} XL isotope ratio mass spectrometer (IRMS) (Thermo Fisher Scientific). The $^{13}C/^{12}C$ of CH_4 in natural gas was measured with a Flash EA1112 elemental analyzer (Thermo Fisher Scientific) that was connected to a Delta V Advantage IRMS with a Conflo IV interface (Thermo Fisher Scientific). Stable isotope ratios were expressed in the conventional δ notation calculated from the equation:

$$\delta = [R_{sample}/R_{standard} - 1] \times 1000 \, [‰],$$

where R is the isotope ratio (D/H, $^{18}O/^{16}O$, or $^{13}C/^{12}C$). All isotope ratios are reported relative to international standards: Vienna Standard Mean Ocean Water for δD and $\delta^{18}O$, and Vienna Pee Dee Belemnite

for δ¹³C. The standard deviations of δD and δ¹⁸O in groundwater and δ¹³C of DIC and CH₄ were ±0.5‰, ±0.1‰, ±1‰, and ±0.3‰, respectively.

Total cell count and catalyzed reporter deposition fluorescence in situ *hybridization (CARD-FISH)*

Groundwater samples for the total cell count and CARD-FISH analysis were filtered using polycarbonate membrane filters (pore size, 0.2 μm; diameter, 25 mm) (Millipore, Billerica, MA, USA). In the total cell count, microbial cells trapped on the filters were stained with SYBR Green I (Life Technologies, Carlsbad, CA, USA) (55). Stained cells were observed under a BX51 epifluorescence microscope equipped with a U-MNIB3 fluorescence filter (Olympus, Tokyo, Japan), and more than 20 microscopic fields were counted for each sample. Cell counting was performed within 48 h of groundwater sampling.

A CARD-FISH analysis targeting prokaryotic 16S rRNAs was conducted with minor modifications to the protocol described by Matsushita *et al.* (32). Briefly, microbial cells collected on the filter were fixed in 3% paraformaldehyde at 4°C for 1 h and dehydrated in 50, 80, and 99.5% ethanol solutions for 3 min each time. Cell fixation was conducted within 12 h of groundwater sampling. The filter was incubated in a lysozyme solution (5 mg mL⁻¹ in 1 mM EDTA, 10 mM Tris-HCl, and 10 mM NaCl) at 37°C for 1 h for cell wall permeabilization. Hybridization was conducted using the following horseradish peroxidase-labeled probes: *Archaea*-specific ARCH915 (45), *Bacteria*-specific EUB338 (3), *Methanobacteriales*-specific MB1174 (39), *Methanomicrobiales*-specific MG1200 (39), *Methanosarcinales*-specific MSMX860 (39), and the control probe Non338 (51) with hybridization buffer described by Mitsunobu *et al.* (34) (35% formamide concentration). The Cy3-labeled tyramide signal was amplified using the TSA-Plus cyanine 3 system (Perkin Elmer, Waltham, MA, USA). All microbial cells were counterstained with SYBR Green I (Life Technologies). Stained cells were observed under a model BX51 epifluorescence microscope (Olympus) equipped with a U-MNIB3 filter (Olympus) for SYBR Green I-stained cells and a U-MWIG3 filter (Olympus) for FISH-positive cells, and more than 20 microscopic fields were counted for each sample.

Next generation sequencer (NGS) analysis of archaeal and bacterial 16S rRNA genes

In order to analyze archaeal and bacterial populations in groundwater samples, 10 L of each groundwater sample was aseptically filtered using Sterivex-GV filter units (pore size, 0.22 μm) (Millipore). Bulk DNA was extracted from microbial cells trapped on the filter using the MORA-Extract kit (Kyokuto Pharmaceutical, Tokyo, Japan). The V3–V4 region of archaeal and bacterial 16S rRNA genes was simultaneously amplified from bulk DNA by PCR using the primer set, Pro341F and Pro806R (48). Library generation and sequencing using an Illumina MiSeq sequencer were performed according to the method described by Takahashi *et al.* (48). The Ribosomal Database Project Classifier version 2.10 was used to analyze sequence reads (confidence threshold of 80%) (52). Sequence reads were grouped into operational taxonomic units (OTUs) sharing more than 97% sequence similarity, and then the coverage, Chao 1, and Shannon index were calculated using the Quantitative Insights Into Microbial Ecology version 1.5.0 pipeline (10).

Anaerobic culture of microbial communities in groundwater

Thirty milliliters of each groundwater sample was anaerobically injected into an autoclaved 70-mL serum bottle that was tightly sealed with a sterile butyl-rubber stopper and aluminum crimp. In order to assess the potential for CH₄ production by methanogenic archaea, groundwater samples were amended with acetate (20 mM), methanol (20 mM), formate (20 mM), or H₂/CO₂ (80:20, v/v; 150 kPa). Except in the case of H₂/CO₂ amended bottles, the headspaces of the serum bottles were filled with pure N₂ at 150 kPa. These cultures were anaerobically incubated without shaking at the temperatures of the groundwater samples measured at the outflow of the wells.

In order to measure the potential for H₂ and CO₂ production by H₂-producing fermentative bacteria, groundwater samples were amended with 3 mL of YPG medium (10 g yeast extract, 10 g peptone, and 2 g glucose L⁻¹ distilled water) and 2-bromoethanesulfonate (BES, 20 mM), a methanogenesis inhibitor (18). The headspaces of the serum bottles were filled with pure N₂ at 150 kPa, and these cultures were anaerobically incubated without shaking at the temperatures of the groundwater samples measured at the outflow of the wells.

In order to assess the potential for CH₄ production by a syntrophic consortium of H₂-producing fermentative bacteria and H₂-utilizing methanogenic archaea, groundwater samples were amended with 3 mL of YPG medium. As a killed control, groundwater samples were autoclaved and then amended with 3 mL of YPG medium. The headspaces of the serum bottles were filled with pure N₂ at 150 kPa, and these cultures were anaerobically incubated without shaking at the temperatures of the groundwater samples measured at the outflow of the wells.

All cultures were performed in duplicate. H₂, N₂, CH₄, and CO₂ concentrations in the headspaces were measured on a GC-2014 gas chromatograph equipped with a thermal conductivity detector (Shimadzu) as described above.

Archaeal and bacterial 16S rRNA genes in the cultures in which CH₄ production was observed were analyzed according to the clone library method. Briefly, cells in the cultures were collected by centrifugation and lysed by lysozyme and proteinase K. Bulk DNA was purified using both phenol/chloroform/isoamyl alcohol and chloroform/isoamyl alcohol and concentrated with ethanol precipitation. Archaeal and bacterial 16S rRNA gene fragments were amplified by PCR from bulk DNA using the *Archaea*-specific primer set, 109aF and 915aR (17, 45), and *Bacteria*-specific primer set, 8bF and 1512uR (14). The sequences of the inserted PCR products selected from recombinant colonies were elucidated with an Applied Biosystems 3730xl DNA analyzer (Life Technologies). A 3% distance level between sequences was considered the cut-off for distinguishing distinct OTUs. The nearest relative of each OTU was identified using the BLAST program (2), and neighbor-joining phylogenetic trees were then constructed using the CLUSTAL X version 2.1 program (29).

Nucleotide sequence accession numbers

The 16S rRNA gene sequences obtained in the present study have been deposited under DDBJ/ENA/GenBank accession numbers LC179566 to LC179584 and DRA005250.

Results

Physicochemical parameters of groundwater and natural gas

The temperature and pH of groundwater samples measured at the outflow of the wells ranged between 40.7 and 53.7°C and between 7.1 and 7.8, respectively (Table 1). The ORP of groundwater ranged between −275 and −179 mV, suggesting anoxic conditions in deep aquifers. The EC, an indicator of salinity, ranged between 878 and 4,500 mS m⁻¹. The highest concentrations of Na⁺, Ca²⁺, Mg²⁺, NH₄⁺, Cl⁻, Br⁻, I⁻, SO₄²⁻, and DOC were detected in the groundwater sample from the YHN site (Table S2). The concentrations of DOC and HCO₃⁻ ranged between <0.3 and 17 mg L⁻¹ and between 100 and 450 mg L⁻¹, respectively. PO₄³⁻, NO₃⁻, S²⁻, acetate, and formate were below the limits of detection.

The natural gas samples collected from all sites consisted mainly of CH₄ (Table 1). The other principal components of natural gas samples were N₂ and C₂H₆. C₃H₈ was only detected in the natural gas samples collected from YHN. The hydrocarbon gas composition C₁/(C₂+C₃) of the natural gas

Table 1. Physicochemical parameters of groundwater and components of natural gas.

Site code	Groundwater				Natural gas				
	Temp. (°C)	pH	ORP (mV)	EC (mS m^{-1})	N$_2$ (vol.%)	CH$_4$ (vol.%)	C$_2$H$_6$ (vol.%)	C$_3$H$_8$ (vol.%)	C$_1$/(C$_2$ + C$_3$)
YHN	53.7	7.1	−275	4,500	0.24	99.7	0.044	0.003	2,117
LSH	40.7	7.4	−179	3,200	5.94	94.0	0.012	<0.001	7,902
XTU	49.8	7.5	−223	3,090	6.20	93.8	0.019	<0.001	5,031
ARM	41.5	7.8	−250	878	6.25	93.7	0.013	<0.001	7,037

Abbreviations: ORP, oxidation-reduction potential; EC, electrical conductivity; C$_1$, CH$_4$; C$_2$, C$_2$H$_6$; C$_3$, C$_3$H$_8$.

samples (C$_1$, CH$_4$; C$_2$, C$_2$H$_6$; C$_3$, C$_3$H$_8$) ranged between 2,117 and 7,902. The concentrations of H$_2$, O$_2$, CO$_2$, and C$_4$H$_{10}$ were below the limits of detection.

Stable isotopic signatures of groundwater and natural gas

The δD and δ^{18}O of groundwater samples ranged between −24.3‰ and −5.8‰ and between −3.3‰ and 0.6‰, respectively (Table S3). In order to estimate the origin of groundwater in deep aquifers, we plotted these δD and δ^{18}O values in a δD versus δ^{18}O diagram with those of normal seawater, ancient seawater (31), and local surface water (1) and the global meteoric water line (11) (Fig. 2). In this diagram, groundwater collected from YHN was plotted closer to ancient seawater. On the other hand, groundwater from ARM was plotted closer to local surface water. Groundwater from XTU and LSH had similar isotopic signatures and fell on the right region of the global meteoric water line, showing a large δ^{18}O enrichment.

The δ^{13}C of DIC in groundwater (δ^{13}C$_{DIC}$) ranged between −8.64‰ and 3.70‰ (Table S3). The δ^{13}C of CH$_4$ in natural gas (δ^{13}C$_{CH4}$) ranged between −57.2‰ and −36.6‰. The carbon isotope fractionation (α$_c$) between δ^{13}C$_{DIC}$ and δ^{13}C$_{CH4}$ was 1.042–1.052. In order to estimate the origin of CH$_4$ in natural gas samples, we plotted stable isotopic values on the δ^{13}C$_{DIC}$ versus δ^{13}C$_{CH4}$ diagram described by Smith and Pallasser

(44). In this diagram, all samples fell within the boundary between a biogenic origin (α$_c$=1.06–1.08) and thermogenic origin (α$_c$=1.02–1.04), suggesting that all natural gas samples contained CH$_4$ of a mixture of biogenic and thermogenic origins (Fig. 3A). We also used a δ^{13}C$_{CH4}$ versus hydrocarbon gas composition C$_1$/(C$_2$+C$_3$) diagram according to Bernard *et*
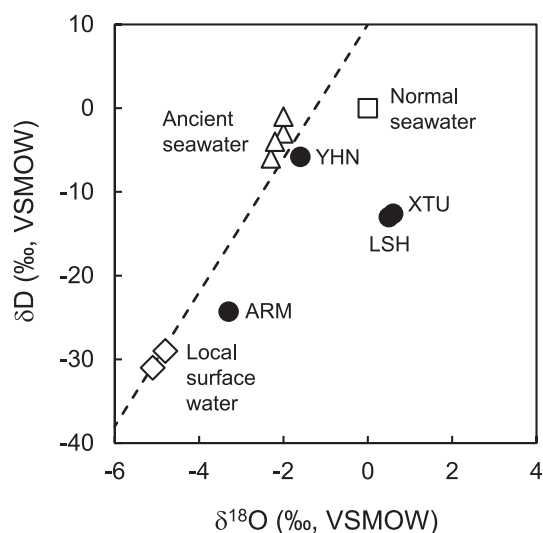

Fig. 2. Stable hydrogen and oxygen isotopic composition of groundwater samples along with those of normal seawater (□), ancient seawater (△), and local surface water (◇). The δD and δ^{18}O values of local surface water and ancient seawater were as reported by Agate *et al.* (1) and Maekawa *et al.* (31), respectively. The broken line represents the global meteoric water line (11).
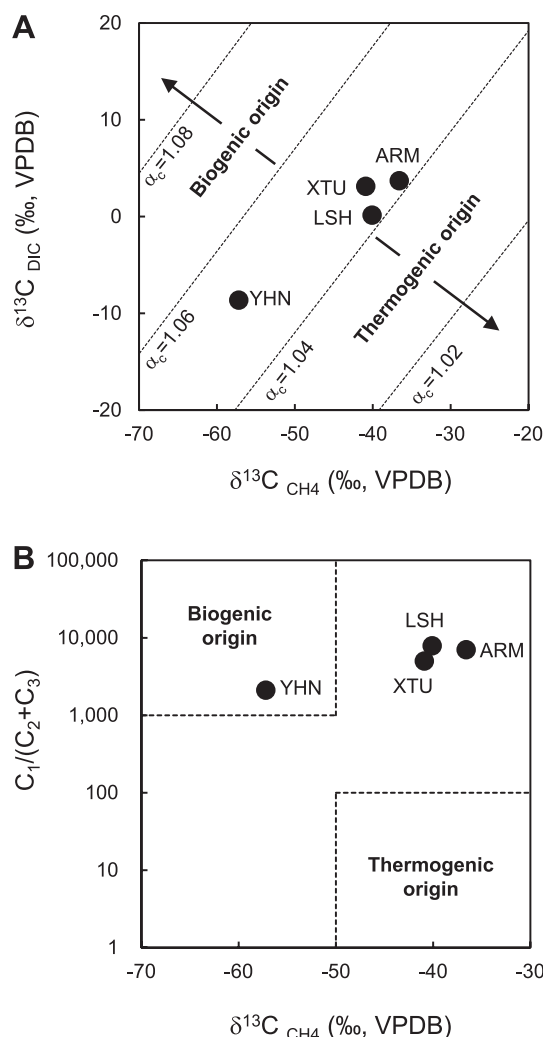
Fig. 3. (A) Stable carbon isotope composition of CH$_4$ in natural gas samples and dissolved inorganic carbon (DIC) in groundwater samples. The categorization of CH$_4$ origins was made according to Smith and Pallasser (45). Dashed lines: equal carbon isotopic fractionation, α$_c$=(δ^{13}C$_{DIC}$+10^3)/(δ^{13}C$_{CH4}$+10^3), for α$_c$=1.02, 1.04, 1.06, and 1.08. (B) Stable carbon isotope composition of CH$_4$ and hydrocarbon gas composition C$_1$/(C$_2$+C$_3$) in natural gas samples. CH$_4$ origins were categorized according to Bernard *et al.* (7). VPDB, Vienna Pee Dee Belemnite.

Table 2. Microbial cell density and relative abundance of FISH-positive cells in groundwater.

Site code	Microbial cell density (cells mL⁻¹)	FISH-positive cells[a]					
		Archaea (%)	*Bacteria* (%)	*Bacteria/Archaea*	*Methanobacteriales* (%)	*Methanomicrobiales* (%)	*Methanosarcinales* (%)
YHN	3.4×10^3	n.d.	n.d.	no data	n.d.	n.d.	n.d.
LSH	1.2×10^5	3.7	4.8	1.3	n.d.	n.d.	n.d.
XTU	1.2×10^5	17.4	21.6	1.2	n.d.	n.d.	n.d.
ARM	4.9×10^4	13.4	33.1	2.5	5.9	n.d.	n.d.

Abbreviation: n.d., not detected.
[a] The relative abundance of FISH-positive cells was assessed by the count ratio of FISH-positive cells to SYBR Green I-stained cells.

al. (7) in order to estimate the origin of CH₄ in natural gas samples. In this diagram, the sample from YHN fell within the region of a biogenic origin (Fig. 3B). On the other hand, all other samples fell within the boundary between biogenic and thermogenic origins.

Abundance of microbial cells in groundwater

Microbial cell densities in anaerobic groundwater samples ranged between 3.4×10^3 and 1.2×10^5 cells mL⁻¹ (Table 2). In order to detect archaeal and bacterial cells in groundwater samples, we conducted a CARD-FISH analysis targeting archaeal and bacterial 16S rRNAs. FISH-positive archaeal and bacterial cells were detected in groundwater samples from LSH, XTU, and ARM (Fig. S1 and S2), and ranged between 3.7% and 17.4% and between 4.8% and 33.1% of all microbial cells, respectively (Table 2). The ratio of FISH-positive bacterial cells to archaeal cells (*Bacteria*/*Archaea*) was 1.2–2.5. The detection of FISH-positive cells in groundwater obtained from YHN was not possible due to the high autofluorescence of mineral particles in the sample.

In order to detect the cells of methanogenic archaea in groundwater samples, we also performed a CARD-FISH analysis targeting 16S rRNAs specific for the archaeal members of the orders *Methanobacteriales*, *Methanomicrobiales*, and *Methanosarcinales*. FISH-positive *Methanobacteriales* cells were detected in the groundwater obtained from ARM (Fig. S3), and constituted 5.9% of all microbial cells (Table 2). On the other hand, FISH-positive *Methanobacteriales* cells were not confirmed in groundwater from LSH and XTU despite several attempts. FISH-positive *Methanomicrobiales* and *Methanosarcinales* cells were not detected in any of the groundwater samples.

Microbial community structures in groundwater

In order to identify microbial community structures in groundwater samples, we performed a NGS analysis targeting archaeal and bacterial 16S rRNA genes. We obtained 14,005–51,920 reads and 196–504 OTUs (Table S4). Coverage reached >99.4%. The Chao1 and Shannon index were 231–742 and 2.97–5.62, respectively.

Archaeal 16S rRNA genes accounted for 1.5%–74.0% of the total reads obtained from each sample (Fig. S4). A phylogenetic analysis of the archaeal 16S rRNA genes revealed the predominance of H₂-utilizing methanogens belonging to the order *Methanobacteriales* in groundwater samples from YHN, XTU, and ARM (Fig. 4A) (56). In LSH, the presence of *Methanobacteriales* was also confirmed. However, most of the archaeal 16S rRNA genes were unclassified archaea. H₂-
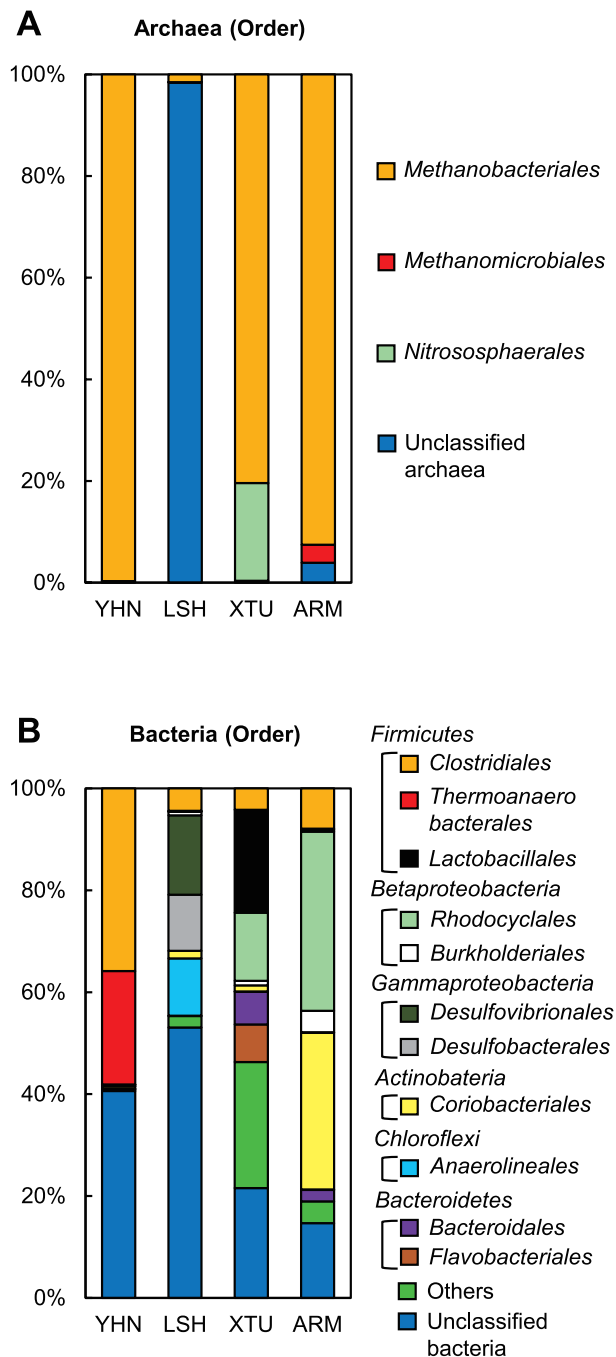
Fig. 4. Archaeal and bacterial assemblages in groundwater samples. (A) The relative abundance (%) of archaeal communities. (B) The relative abundance (%) of bacterial communities.

utilizing methanogens belonging to the order *Methanomicrobiales* were only identified in ARM (42).

An analysis of bacterial 16S rRNA genes demonstrated the presence of bacterial groups that belong to the phyla *Firmicutes*, *Proteobacteria*, *Actinobacteria*, *Chloroflexi*, and *Bacteroidetes* in groundwater samples from each site (Fig. 4B). Bacterial 16S rRNA genes closely related to *Clostridiales*, a bacterial order that belongs to the *Firmicutes*, were detected in all sites. The orders *Thermoanaerobacterales* and *Lactobacillales*, which are the other members of *Firmicutes*, were mainly identified in YHN and XTU, respectively. The bacterial 16S rRNA genes closely related to the bacterial groups of *Gammaproteobacteria* and *Chloroflexi* were detected in LSH. The bacterial groups of *Betaproteobacteria* and *Actinobacteria* were mainly identified in ARM. The presence of *Bacteroidetes* was shown in XTU and ARM.

Potential for biogas production by microbial communities

In order to assess the potential for CH_4 production by methanogenic archaea in the deep aquifers, we anaerobically incubated groundwater samples amended with methanogenic substrates: acetate, methanol, formate, or H_2/CO_2. However, CH_4 production was not observed in these cultures over 75 d of incubation (data not shown).

We then performed anaerobic cultivations using groundwater samples amended with YPG medium and BES to assess the potential for H_2 and CO_2 production mediated by H_2-producing fermentative bacteria. As a result, H_2 and CO_2 were detected in the gas phase of cultures using groundwater samples from all sites (Fig. 5A). In the cultures using groundwater from LSH and XTU, the production of H_2 and CO_2 was observed within 3 d. In the cultures using groundwater from

YHN and ARM, H_2 and CO_2 were detected after 7 and 14 d, respectively.

A high potential for CH_4 production was confirmed in the cultures using groundwater samples amended with YPG medium (Fig. 5B). H_2 and CO_2 production was observed in all cultures within 7 d. After H_2 and CO_2 production, the concentration of H_2 decreased to below the limit of detection. CH_4 production was observed after H_2 levels began to fall. These dynamics of H_2 and CH_4 were similar to those observed previously in syntrophic co-cultures of H_2-producing fermentative bacteria and H_2-utilizing methanogenic archaea (4, 27, 32). In the cultures using groundwater from YHN and LSH, CH_4 production was observed within 10 d. In the cultures using groundwater from XTU and ARM, CH_4 was detected after 14 d. In a killed control using autoclaved groundwater samples amended with YPG medium, H_2 and CH_4 production was not observed over 75 d (data not shown).

In order to identify prokaryotes that generated biogas (*i.e.*, H_2, CO_2, and CH_4) in the cultures using YPG-amended groundwater, we constructed archaeal and bacterial 16S rRNA gene clone libraries. The 16S rRNA gene analysis suggested that H_2-utilizing methanogenic archaea and H_2-producing fermentative bacteria were predominant in the microbial population (Table S5) and were related to the archaeal order *Methanobacteriales* (Fig. S5) and bacterial orders *Bacillales*, *Synergistales*, *Clostridiales*, and *Thermotogales* (Fig. S6) (12, 30, 40, 53).

Discussion

The anaerobic groundwater sample collected from the YHN site had a similar EC value and Na$^+$ and Cl$^−$ concentra-
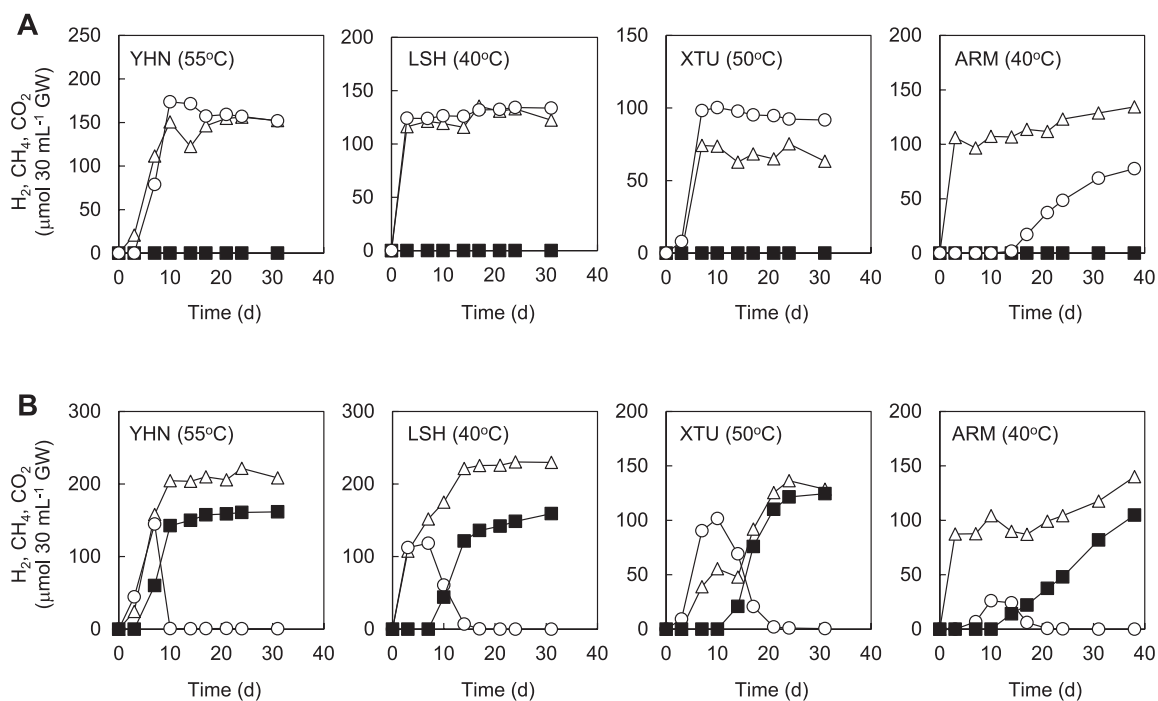

Fig. 5. Biogas production from groundwater samples amended with (A) YPG medium and BES and (B) YPG medium incubated at temperatures of groundwater samples measured at the outflow of the well. Cumulative measurements in the gas phase of bottled cultures are shown as follows: H_2 (○); CH_4 (■); and CO_2 (△). Incubation temperatures are shown in parentheses. Although representative results of cultures performed in duplicate are shown, the other culture showed a similar potential for biogas production.

tions as normal seawater (Tables 1 and S2). The groundwater sample also had high levels of I^- and Br^-. These chemical features are consistent with those of ancient seawater, which is comprised of groundwater that originated from seawater and was maintained for a long period in a low-temperature deep aquifer (24). Additionally, the δD and $\delta^{18}O$ values of the groundwater sample were consistent with those of ancient seawater (Fig. 2). Therefore, the groundwater in the YHN deep aquifer appeared to have originated from seawater that was conserved in the deep aquifer over a long period at a relatively low temperature. In contrast, groundwater from the ARM site had the lowest EC value (Table 1) and showed similar δD and $\delta^{18}O$ signatures to those of local surface water (Fig. 2). These characteristics suggest that the ARM deep aquifer has mainly been affected by rainwater infiltrating from surface environments. Groundwater from the LSH and XTU sites had similar chemical and isotopic signatures. The EC value of groundwater was approximately 60% of that of normal seawater (approximately 5,000 mS m⁻¹), suggesting that groundwater originated from a mixture of seawater and rainwater (Table 1). The $\delta^{18}O$ values of the groundwater samples were higher than that of normal seawater sample (Fig. 2). These high $\delta^{18}O$ values suggest that groundwater in these deep aquifers was affected by water-rock interactions in high-temperature deep subterranean environments (9).

CH_4 was the predominant component of natural gas samples collected from all sites (Table 1). In the present study, we estimated the origin of CH_4 in natural gas samples using a $\delta^{13}C_{DIC}$ versus $\delta^{13}C_{CH4}$ diagram and $\delta^{13}C_{CH4}$ versus $C_1/(C_2+C_3)$ diagram (Fig. 3). These chemical and stable carbon isotopic signatures of groundwater and natural gas samples suggested that CH_4 in the natural gas samples was of a biogenic origin or a mixture of biogenic and thermogenic origins.

The microbial cell densities in groundwater samples were consistent with those previously reported in deep aquifers associated with the Paleogene accretionary prism (27, 32). The CARD-FISH analysis targeting archaeal 16S rRNA detected metabolically active archaeal cells in groundwater samples from LSH, XTU, and ARM (Table 2). Additionally, we successfully detected FISH-positive *Methanobacteriales* cells, known as H_2-utilizing methanogenic archaea, in the groundwater from ARM. The NGS analysis of archaeal 16S rRNA genes revealed the presence of *Methanobacteriales* in the groundwater from all sites (Fig. 4A). In contrast, methanogenic archaea that use acetate or methanol as methanogenic substrates were not confirmed. These results suggest that H_2-utilizing methanogenesis is a main microbial CH_4 production pathway in the deep aquifers tested. However, the potential for CH_4 production by H_2-utilizing methanogens was not confirmed in the cultures using groundwater samples amended with H_2/CO_2. This may have been due to the growth inhibition of H_2-utilizing methanogens caused by a shortage of inorganic nutrients, such as phosphate, vitamin, and trace elements, or by a high concentration of H_2 and CO_2 (41).

Although archaeal 16S rRNA genes closely related to the order *Methanobacteriales* were obtained from all sites (Fig. 4A), FISH-positive *Methanobacteriales* cells were only detected from ARM (Table 2). This result may have been due to the low abundance of *Methanobacteriales* cells in groundwater samples or a mismatch between the probe used in the present study and their 16S rRNA sequences.

The NGS analysis targeting bacterial 16S rRNA genes revealed the presence of bacteria belonging to *Firmicutes* in all groundwater samples (Fig. 4B). These bacteria are generally known to have the ability to degrade organic matter to H_2 and CO_2 by fermentation (21, 28, 30). Additionally, the members of the bacterial groups belonging to *Betaproteobacteria*, *Gammaproteobacteria*, *Actinobacteria*, *Chloroflexi*, and *Bacteroidetes*, which were also identified in each site, have been shown to possess the ability to grow by fermentation under anaerobic environments (5, 6, 20, 37, 54). We confirmed a high potential for H_2 and CO_2 production by H_2-producing fermentative bacteria in the cultures using groundwater samples amended with YPG medium and BES (Fig. 5A). Therefore, these bacteria are considered to grow by fermentation and degrade organic matter to H_2 and CO_2 in the deep aquifers.

The H_2-utilizing methanogenic archaea and H_2-producing fermentative bacteria identified in the present study have frequently been found in subsurface oil reservoirs, natural gas reservoirs, and coal deposits in which microbial CH_4 production has been observed (32, 33). Additionally, it is generally known that a syntrophic consortium of H_2-producing fermentative bacteria and H_2-utilizing methanogenic archaea leads to the biodegradation of organic matter to CH_4 in anaerobic environments (38, 41). In the present study, a high potential for CH_4 production by a syntrophic consortium of H_2-producing fermentative bacteria and H_2-utilizing methanogenic archaea was demonstrated by the cultures using groundwater samples amended with YPG medium (Fig. 5B). The potential for microbial CH_4 production was similar to that previously reported in deep aquifers of the Paleogene accretionary prism (27, 32). The predominance of H_2-utilizing methanogenic archaea and H_2-producing fermentative bacteria in the cultures was also confirmed by the 16S rRNA gene analysis (Table S6). Although the predominant fermentative bacteria in the cultures belonged to the orders *Bacillales*, *Synergistales*, *Clostridiales*, and *Thermotogales*, except for *Clostridiales*, these bacterial groups were rarely found in natural groundwater samples (Fig. 4B). This may have been due to the strong selective pressure caused by using very high concentrations of organic substrates.

Our geochemical and microbiological data strongly suggest the presence of a CH_4 production process by a syntrophic consortium of H_2-producing fermentative bacteria and H_2-utilizing methanogenic archaea in deep aquifers of the Cretaceous accretionary prism in Okinawa Island, Japan. The microbial activity and CH_4 production process revealed in this study were similar to those previously reported in deep aquifers of the Paleogene accretionary prism (27, 32). Since accretionary prisms are derived from ancient marine sediments scraped from the subducting ocean plate, the sediments contain layers of mudstone rich in complex organic matter (8, 22). This organic matter is considered to support the activity of a microbial community that generates CH_4 in deep aquifers. Taken together, our results suggest that the ongoing biodegradation of organic matter makes a major contribution to CH_4 production in deep aquifers of the Cretaceous accretionary prism as well as those of the Paleogene accretionary prism.

References

1. Agata, S., H. Satake, and A. Tokuyama. 2001. Chemical characteristics and isotopic compositions of spring and river waters in Okinawa Island. Chikyu Kagaku (Nippon Chikyu Kagakkai) 35:27–41 (in Japanese with an English abstract).
2. Altschul, S.F., T.L. Madden, A.A. Schäffer, J. Zhang, Z. Zhang, W. Miller, and D.J. Lipman. 1997. Gapped BLAST and PSI-BLAST: a new generation of protein database search programs. Nucleic Acids Res. 25:3389–3402.
3. Amann, R.I., L. Krumholz, and D.A. Stahl. 1990. Fluorescent-oligonucleotide probing of whole cells for determinative, phylogenetic, and environmental studies in microbiology. J. Bacteriol. 172:762–770.
4. Baito, K., S. Imai, M. Matsushita, M. Otani, Y. Sato, and H. Kimura. 2015. Biogas production using anaerobic groundwater containing a subterranean microbial community associated with the accretionary prism. Microb. Biotechnol. 8:837–845.
5. Bale, S.J., K. Goodman, P.A. Rochelle, J.R. Marchesi, J.C. Fry, A.J. Weightman, and R.J. Parkes. 1997. *Desulfovibrio profundus* sp. nov., a novel barophilic sulfate-reducing bacterium from deep sediment layers in the Japan Sea. Int. J. Syst. Bacteriol. 47:515–521.
6. Benno, Y., J. Watabe, and T. Mitsuoka. 1983. *Bacteroides pyogenes* sp. nov., *Bacteroides suis* sp. nov., and *Bacteroides helcogenes* sp. nov., new species from abscesses and feces of pigs. Syst. Appl. Microbiol. 4:396–407.
7. Bernard, B.B., J.M. Brooks, and W.M. Sackett. 1978. Light hydrocarbons in recent Texas continental shelf and slope sediments. J. Geophys. Res. 83:4053–4061.
8. Berner, U., and J. Koch. 1993. Organic matter in sediments of site 808, Nankai accretionary prism, Japan. Proc. Ocean Drill. Program: Sci. Results 131:379–385.
9. Bowers, T.S., and H.P. Taylor. 1985. An integrated chemical and stable-isotope model of the origin of midocean ridge hot spring systems. J. Geophys. Res. 90:12583–12606.
10. Caporaso, J.G., J. Kuczynski, J. Stombaugh, *et al.* 2010. QIIME allows analysis of high-throughput community sequencing data. Nat. Methods 7:335–336.
11. Craig, H. 1961. Isotopic variations in meteoric waters. Science 133:1702–1703.
12. Dahle, H., and N.K. Birkeland. 2006. *Thermovirga lienii* gen. nov., sp. nov., a novel moderately thermophilic, anaerobic, amino-acid-degrading bacterium isolated from a North Sea oil well. Int. J. Syst. Evol. Microbiol. 56:1539–1545.
13. Dawson, K.S., M.R. Osburn, A.L. Sessions, and V.J. Orphan. 2015. Metabolic associations with archaea drive shifts in hydrogen isotope fractionation in sulfate-reducing bacterial lipids in cocultures and methane seeps. Geobiology 13:462–477.
14. Eder, W., W. Ludwig, and R. Huber. 1999. Novel 16S rRNA gene sequences retrieved from highly saline brine sediments of Kebrit Deep, Red Sea. Arch. Microbiol. 172:213–218.
15. Fagereng, Å. 2011. Fractal vein distributions within a fault-fracture mesh in an exhumed accretionary mélange, Chrystalls Beach Complex, New Zealand. J. Struct. Geol. 33:918–927.
16. Geological Survey of Japan, AIST (ed.). 2014. Seamless digital geological map of Japan 1: 200,000. Jan 14, 2014 version. Geological Survey of Japan. National Institute of Advanced Industrial Science and Technology, Ibaraki, Japan.
17. Großkopf, R., P.H. Janssen, and W. Liesack. 1998. Diversity and structure of the methanogenic community in anoxic rice paddy soil microcosms as examined by cultivation and direct 16S rRNA gene sequence retrieval. Appl. Environ. Microbiol. 64:960–969.
18. Gunsalus, R.P., J.A. Romesser, and R.S. Wolfe. 1978. Preparation of coenzyme M analogs and their activity in the methyl coenzyme M reductase system of *Methanobacterium thermoautotrophicum*. Biochemistry 17:2374–2377.
19. Hervé, F., M. Calderón, C.M. Fanning, R.J. Pankhurst, and E. Godoy. 2013. Provenance variations in the Late Paleozoic accretionary complex of central Chile as indicated by detrital zircons. Gondwana Res. 23:1122–1135.
20. Hiraishi, A., Y. Hoshino, and T. Satoh. 1991. *Rhodoferax fermentans* gen. nov., sp. nov., a phototrophic purple nonsulfur bacterium previously referred to as the "*Rhodocyclus gelatinosus*-like" group. Arch. Microbiol. 155:330–336.
21. Kandler, O., U. Schillinger, and N. Weiss. 1983. *Lactobacillus bifermentans* sp. nov., nom. rev., an organism forming CO_2 and H_2 from lactic acid. Syst. Appl. Microbiol. 4:408–412.
22. Kaneko, M., H. Shingai, J.W. Pohlman, and H. Naraoka. 2010. Chemical and isotopic signature of bulk organic matter and hydrocarbon biomarkers within mid-slope accretionary sediments of the northern Cascadia margin gas hydrate system. Mar. Geol. 275:166–177.
23. Kano, K., M. Nakaji, and S. Takeuchi. 1991. Asymmetrical melange fabrics as possible indicators of the convergent direction of plates: a case study from the Shimanto Belt of the Akaishi Mountains, central Japan. Tectonophysics 185:375–388.
24. Katayama, T., H. Yoshioka, Y. Muramoto, J. Usami, K. Fujiwara, S. Yoshida, Y. Kamagata, and S. Sakata. 2015. Physicochemical impacts associated with natural gas development on methanogenesis in deep sand aquifers. ISME J. 9:436–446.
25. Kato, S., T. Honda, and K. Omijya. 2012. Petroleum geology of the Nanjo R1 exploratory well, Okinawa Prefecture. J. Jpn. Assoc. Pet. Technol. 77:86–95 (in Japanese with an English abstract).
26. Kemkin, I.V., and A.N. Filippov. 2001. Structure and genesis of the lower structural unit of the Samarka Jurassic accretionary prism (Sikhote-Alin, Russia). Geodiversitas 23:323–339.
27. Kimura, H., H. Nashimoto, M. Shimizu, S. Hattori, K. Yamada, K. Koba, N. Yoshida, and K. Kato. 2010. Microbial methane production in deep aquifer associated with the accretionary prism in Southwest Japan. ISME J. 4:531–541.
28. Kublanov, I.V., M.I. Prokofeva, N.A. Kostrikina, T.V. Kolganova, T.P. Tourova, J. Wiegel, and E.A. Bonch-Osmolovskaya. 2007. *Thermoanaerobacterium aciditolerans* sp. nov., a moderate thermoacidophile from a Kamchatka hot spring. Int. J. Syst. Evol. Microbiol. 57:260–264.
29. Larkin, M.A., G. Blackshields, N.P. Brown, *et al.* 2007. Clustal W and Clustal X version 2.0. Bioinformatics 23:2947–2948.
30. Liu, C., S.M. Finegold, Y. Song, and P.A. Lawson. 2008. Reclassification of *Clostridium coccoides*, *Ruminococcus hansenii*, *Ruminococcus hydrogenotrophicus*, *Ruminococcus luti*, *Ruminococcus productus* and *Ruminococcus schinkii* as *Blautia coccoides* gen. nov., comb. nov., *Blautia hansenii* comb. nov., *Blautia hydrogenotrophica* comb. nov., *Blautia luti* comb. nov., *Blautia producta* comb. nov., *Blautia schinkii* comb. nov. and description of *Blautia wexlerae* sp. nov., isolated from human faeces. Int. J. Syst. Evol. Microbiol. 58:1896–1902.
31. Maekawa, T., S. Igari, and N. Kaneko. 2006. Chemical and isotopic compositions of brines from dissolved-in-water type natural gas fields in Chiba, Japan. Geochem. J. 40:475–484.
32. Matsushita, M., S. Ishikawa, K. Nagai, Y. Hirata, K. Ozawa, S. Mitsunobu, and H. Kimura. 2016. Regional variation of CH_4 and N_2 production processes in the deep aquifers of an accretionary prism. Microbes Environ. 31:329–338.
33. Meslé, M., G. Dromart, and P. Oger. 2013. Microbial methanogenesis in subsurface oil and coal. Res. Microbiol. 164:959–972.
34. Mitsunobu, S., F. Shiraishi, H. Makita, B.N. Orcutt, S. Kikuchi, B.B. Jorgensen, and Y. Takahashi. 2012. Bacteriogenic Fe(III) (Oxyhydr) oxides characterized by synchrotron microprobe coupled with spatially resolved phylogenetic analysis. Environ. Sci. Technol. 46:3304–3311.
35. Miyagi, N., S. Baba, and R. Shinjo. 2013. Whole-rock chemical composition of the pre-Neogene basement rocks and detritus garnet composition in the Okinawa-jima and neighbor islands. J. Geol. Soc. Jpn. 119:665–678 (in Japanese with an English abstract).
36. Miyajima, T., Y. Yamada, Y.T. Hanba, K. Yoshii, T. Koitabashi, and E. Wada. 1995. Determining the stable isotope ratio of total dissolved inorganic carbon in lake water by GC/C/IRMS. Limnol. Oceanogr. 40:994–1000.

37. Nagai, F., Y. Watanabe, and M. Morotomi. 2010. *Slackia piriformis* sp. nov. and *Collinsella tanakaei* sp. nov., new members of the family *Coriobacteriaceae*, isolated from human faeces. Int. J. Syst. Evol. Microbiol. 60:2639–2646.

38. Noguchi, M., F. Kurisu, I. Kasuga, and H. Furumai. 2014. Time-resolved DNA stable isotope probing links *Desulfobacterales*- and *Coriobacteriaceae*-related bacteria to anaerobic degradation of benzene under methanogenic conditions. Microbes Environ. 29:191–199.

39. Raskin, L., J.M. Stromley, B.E. Rittmann, and D.A. Stahl. 1994. Group-specific 16S ribosomal-rna hybridization probes to describe natural communities of methanogens. Appl. Environ. Microbiol. 60:1232–1240.

40. Ravot, G., M. Magot, M.L. Fardeau, B.K. Patel, G. Prensier, A. Egan, J.L. Garcia, and B. Ollivier. 1995. *Thermotoga elfii* sp. nov., a novel thermophilic bacterium from an African oil-producing well. Int. J. Syst. Evol. Microbiol. 45:308–314.

41. Sakai, S., H. Imachi, Y. Sekiguchi, I.C. Tseng, A. Ohashi, H. Harada, and Y. Kamagata. 2009. Cultivation of methanogens under low-hydrogen conditions by using the coculture method. Appl. Environ. Microbiol. 75:4892–4896.

42. Sakai, S., M. Ehara, I.C. Tseng, T. Yamaguchi, S.L. Brauer, H. Cadillo-Quiroz, S.H. Zinder, and H. Imachi. 2012. *Methanolinea mesophila* sp. nov., a hydrogenotrophic methanogen isolated from rice field soil, and proposal of the archaeal family *Methanoregulaceae* fam. nov. within the order *Methanomicrobiales*. Int. J. Syst. Evol. Microbiol. 62:1389–1395.

43. Sakata, S., T. Maekawa, S. Igari, and Y. Sano. 2012. Geochemistry and origin of natural gases dissolved in brines from gas fields in southwest Japan. Geofluids 12:327–335.

44. Smith, J.W., and R.J. Pallasser. 1996. Microbial origin of Australian coalbed methane. AAPG Bull. 80:891–897.

45. Stahl, D.A., and R. Amann. 1991. Development and application of nucleic acid probes in bacterial systematics, p. 205–248. *In* E. Stackebrandt, and M. Goodfellow (ed.), Nucleic Acid Techniques in Bacterial Systematics. John Wiley & Sons, New York.

46. Taira, A., J. Katto, M. Tashiro, M. Okamura, and K. Kodama. 1988. The Shimanto Belt in Shikoku, Japan: evolution of Cretaceous to Miocene accretionary prism. Mod. Geol. 12:5–46.

47. Taira, A., T. Byrne, and J. Ashi. 1992. Photographic Atlas of an Accretionary Prism: Geologic Structures of the Shimanto Belt, Japan. University of Tokyo Press, Tokyo.

48. Takahashi, S., J. Tomita, K. Nishioka, T. Hisada, and M. Nishijima. 2014. Development of a prokaryotic universal primer for simultaneous analysis of bacteria and archaea using next-generation sequencing. PLoS One 9:e105592.

49. Ujiie, H. 1994. Early Pleistocene birth of the Okinawa Trough and Ryukyu Island Arc at the northwestern margin of the Pacific: evidence from Late Cenozoic planktonic foraminiferal zonation. Palaeogeogr. Palaeoclimatol. Palaeoecol. 108:457–474.

50. Ujiie, K. 2002. Evolution and kinematics of an ancient décollement zone, mélange in the Shimanto accretionary complex of Okinawa Island, Ryukyu Arc. J. Struct. Geol. 24:937–952.

51. Wallner, G., R. Amann, and W. Beisker. 1993. Optimizing fluorescent in situ hybridization with rRNA-targeted oligonucleotide probes for flow cytometric identification of microorganisms. Cytometry 14:136–143.

52. Wang, Q., G.M. Garrity, J.M. Tiedje, and J.R. Cole. 2007. Naïve Bayesian classifier for rapid assignment of rRNA sequences into the new bacterial taxonomy. Appl. Environ. Microbiol. 73:5261–5267.

53. Watanapokasin, R.Y., A. Boonyakamol, S. Sukseree, A. Krajarng, T. Sophonnithiprasert, S. Kanso, and T. Imai. 2009. Hydrogen production and anaerobic decolorization of wastewater containing Reactive Blue 4 by a bacterial consortium of *Salmonella subterranea* and *Paenibacillus polymyxa*. Biodegradation 20:411–418.

54. Yamada, T., Y. Sekiguchi, S. Hanada, H. Imachi, A. Ohashi, H. Harada, and Y. Kamagata. 2006. *Anaerolinea thermolimosa* sp. nov., *Levilinea saccharolytica* gen. nov., sp. nov. and *Leptolinea tardivitalis* gen. nov., sp. nov., novel filamentous anaerobes, and description of the new classes *Anaerolineae classis* nov. and *Caldilineae classis* nov. in the phylum *Chloroflexi*. Int. J. Syst. Evol. Microbiol. 56:1331–1340.

55. Yanagawa, K., A. Tani, N. Yamamoto, A. Hachikubo, A. Kano, R. Matsumoto, and Y. Suzuki. 2016. Biogeochemical cycle of methanol in anoxic deep-sea sediments. Microbes Environ. 31:190–193.

56. Zhu, J., X. Liu, and X. Dong. 2011. *Methanobacterium movens* sp. nov. and *Methanobacterium flexile* sp. nov., isolated from lake sediment. Int. J. Syst. Evol. Microbiol. 61:2974–2978.